PHYSICAL REVIEW B VOLUME 40, NUMBER 6 15 AUGUST 1989-II

Metal/GaP(110) interface formation: Ti, Pd, Ag, and Au adatom deposition

B. M. Trafas, F. Xu,* M. Vos, C. M. Aldao, and J. H. Weaver
Department of Chemical Engineering and Materials Science, University of Minnesota, Minneapolis, Minnesota 55455
(Received 17 April 1989)

The evolution on interfaces formed at 300 K by the deposition of atoms of Ti, Pd, Ag, and Au on cleaved GaP(110) has been studied using synchrotron-radiation photoemission. For Ti, Pd, and Au, metal deposition induces immediate disruption of the substrate and atomic intermixing. In contrast, Ag deposition at 300 K onto GaP(110) leads to cluster formation, and there is no observable surface disruption. Comparison of these results for atom condensation on GaP(110) to those for GaAs(110) and InP(110) indicates that the Ga and P redistribution and the formation of reaction products is indistinguishable, regardless of the particular semiconductor substrate.

INTRODUCTION

Contacts between metals and III-V compound semiconductors have been extensively studied with photoemission, especially for GaAs- and InP-based systems,[1] and the results are complemented by insight gained with a wide variety of other techniques.[2] However, relatively few studies of metal/GaP interface formation have been reported.[3–8] Such studies are of fundamental importance in understanding the physical, chemical, and structural properties of these junctions, and they provide guidelines for the design of devices, multilayers, and composites. Despite substantial progress, the mechanism behind adatom-induced substrate disruption has been elusive, and the understanding of this phenomenon, common for a large class of metal/semiconductor systems, is crucial in the studies of interface formation. Indeed, the conditions of the surface established at low coverage are reflected in subsequent growth and atom distribution.

In this paper, we report results of a detailed synchrotron radiation photoemission study of GaP(110)-based interfaces involving Ti, Pd, Ag, and Au overlayers. These representative metals were chosen in order to focus on interfacial properties for systems which are expected to be reactive (Ti), weakly reactive (Pd and Au), and nonreactive (Ag). Here, we will examine adatom-induced disruption, the subsequent formation of interface reaction products, and segregation of the released semiconductor atoms. We will compare the general trends for Ga and P atoms for GaP(110) with results obtained under equivalent conditions for these same metal overlayers formed on GaAs(110) and InP(110). High-resolution core-level and valence-band results indicate that there is identical behavior for the Ga and P atoms for a particular metal overlayer once surface disruption has been initiated, regardless of the semiconductor.

EXPERIMENTAL

Soft-x-ray photoemission experiments were carried out at the Aladdin electron storage ring at the Wisconsin Synchrotron Radiation Center using the Grasshopper Mark II monochromator and beamline. These measurements emphasize core-level line-shape changes and core-level intensity variations as a function of the amount of metal deposited. Photoelectrons from the Ga $3d$ and P $2p$ core levels and the valence bands were energy analyzed with a double-pass cylindrical mirror analyzer in a vacuum system described in detail elsewhere.[9] The incident photon energies were chosen to give equal inelastic mean free paths λ for Ga $3d$ and P $2p$ photoelectrons [$h\nu=60$ eV for Ga and 170 eV for P in the surface-sensitive mode ($\lambda\sim4$ Å) compared to 40 and 145 eV for the bulk-sensitive mode ($\lambda\sim6$ Å)]. Monochromator slits and analyzer pass energies were chosen to give total energy resolution of ~250 meV for Ga and ~400 meV for P.

Posts of n-type GaP (S doped at 4×10^{17} cm^{-3}) were cleaved *in situ* to produce mirrorlike (110) surfaces. The quality of the cleaves was checked visually and spectroscopically with core-level and valence-band features to assure high-quality surfaces before beginning the interface studies. Adatoms were evaporated from resistively heated tungsten boats that had been thoroughly degassed so that pressures below 2×10^{-10} Torr could be maintained during evaporation. The source to sample distance was ~35 cm and the deposition rate was typically 1 Å per minute, as monitored with a calibrated quartz oscillator. The amount of material deposited will be expressed in angstroms in this paper. The conversion to substrate-equivalent monolayers is 0.60 ML/Å for Ti, 0.71 ML/Å for Pd, 0.62 ML/Å for Au, and 0.62 ML/Å for Ag. This assumes the deposition of one adatom per semiconductor-atom site on the GaP(110) surface where the planar density is 9.52×10^{14} atoms/cm^2. We do not mean, however, to imply epitaxial growth.

Line-shape decompositions of the Ga $3d$ and P $2p$ core-level energy distribution curves (EDC's) were done with a nonlinear least-squares minimization routine[10] on an IBM PC-RT. The convolution of Gaussian and Doniach-Sunjic (DS) functions was used to fit the experimental spectra. Up to three spin-orbit pairs were introduced to account for contributions from atoms in distinguishable chemical environments. These correspond to the substrate, the surface, and the reaction products. Details of the data-analysis procedure can be found in Ref. 11. In general, our fits were obtained by fixing the Lorentzian width, the branching ratio, and the spin-orbit splitting of all the components of a single atomic species

for all coverages at the values determined for the cleaved substrate. However, the Gaussian widths of the adatom-induced features were allowed to vary to account for changes in local bonding. These constraints increased our confidence in the reliability of the fits.

The initial Fermi-level surface position varies considerably from cleave to cleave. This variation appears to be correlated with the quality of the cleave and indicates that the position of the Fermi level at the cleaved (110) surface is dominated by extrinsic rather than intrinsic surface states. Chiaradia *et al.*[8] recently reported that Fermi-level stabilization due to extrinsic surface states occurs over a wide range of positions, most likely because of the cleave-induced defects. In the present study, this uncertainty in initial Fermi-level position has compromised measurements of substrate band bending as a function of metal deposition and hence, we will focus on interface reaction, morphology, and atom distribution in this paper.

RESULTS

Clean GaP(110) surfaces

The bottom-most Ga 3*d* and P 2*p* EDC's of Fig. 1 are for the clean GaP(110) surface. Line-shape analysis reveals two components corresponding to bulk atoms (component 1) and surface-shifted atoms (component 2), as expected by analogy to previous studies of (110) surfaces of III-V compound semiconductors.[12–14] From the intensity ratio of the surface and bulk components, we estimate the probe depth 3λ to be ~ 12 Å at a photon energy of 60 eV for Ga 3*d* and 170 eV for P 2*p*. (Spectra with lower surface sensitivity $3\lambda \simeq 18$ Å at $h\nu = 40$ eV for Ga 3*d* and 145 eV for P 2*p* complement the spectra shown here.) The surface components appear at 0.34 ± 0.03 eV for Ga 3*d* and -0.41 ± 0.03 eV for P 2*p* relative to the bulk components. This is in good agreement with the predictions of Priester *et al.*[14] for GaP(110) and the values recently reported by McLean and Ludeke.[7] Comparison to analogous results for GaAs(110) shows the Ga component to be shifted slightly more for GaP(110) (0.28 eV for GaAs compared to 0.34 for GaP) and results for InP(110) indicate a less-shifted P 2*p* surface component [at -0.30 eV compared to -0.41 for GaP(110)]. These chemical shifts, which probe changes of the electrostatic potential may be understood in a first approximation as a charge transfer between atoms having different electronegativities. Mönch has concluded that GaP(110) has the largest experimental and theoretical charge transfer of the III-V compound semiconductors,[13] and this explains the larger observed chemical shift for GaP(110) compared to InP(110) and GaAs(110).

For cleaved GaP(110), the Ga 3*d* emission could best be fit for $h\nu = 60$ eV with a spin-orbit splitting of 0.44 eV, a branching ratio of 0.70, a Gaussian width of 0.42 eV, and a Lorentzian width of 0.15 eV. For P 2*p* at $h\nu = 170$ eV, the spin-orbit splitting was 0.86 eV, the branching ratio was 0.50, the Gaussian width was 0.63 eV, and Lorentzian width was 0.15 eV. These parameters were then used in analysis of the spectra acquired during interface formation.

Ti/GaP(110)

The Ti/GaP(110) interface is representative of a highly reactive interface, and Fig. 1 summarizes the evolving Ga 3*d* and P 2*p* core-level spectra as a function of Ti deposition. These spectra have been background subtracted and normalized to the same height to emphasize line-shape changes. The binding energies are referenced to the position of the substrate bulk component. Quantitative information about intensity variations for the various features identified in Fig. 1 is given through the attenuation curves of Fig. 2. These were determined by measuring the total integrated core-level emission after deposition of Θ Å of metal with normalization to the emission for the clean GaP(110) surface, namely $\ln[I(\Theta)/I(0)]$.

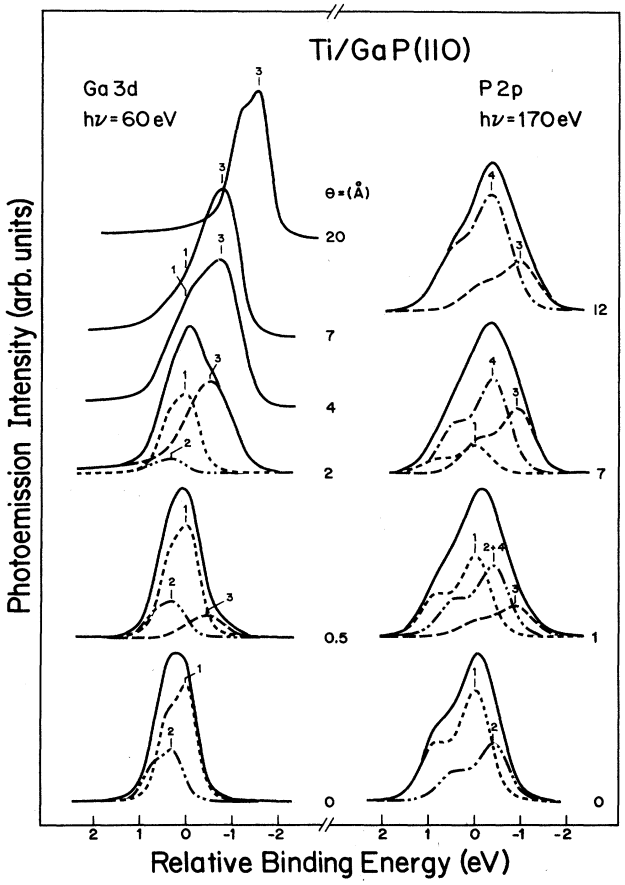

FIG. 1. Ga 3*d* and P 2*p* core-level EDC's for Ti/GaP(110) for representative Ti depositions. The spectra have been background subtracted, normalized to the same height, and aligned according to the substrate bulk component. Also shown are the line-shape decompositions (dashed) representing the different chemical bonding configurations. Component 1 reveals the substrate bulk peak and component 2 reveals the surface-shifted contribution. For Ga 3*d*, component 3 corresponds to dissociated atoms dissolved in the Ti matrix. Component 3 for P 2*p* is a precursor reaction product and component 4 is a Ti-P reaction product.

In such attenuation curves, approximately layer-by-layer metal growth is revealed by a straight line with $1/e$ decay length corresponding to the photoelectron mean free path through the overlayer.

Ga $3d$ line-shape analysis for Ti/GaP(110) indicates that the surface component decreases rapidly and disappears at coverages above ~ 2 Å, suggesting a nearly homogeneous coverage of the surface. Satisfactory line-shape decomposition (as defined as statistically neutral residuals when fits and raw data are compared[11]) for depositions exceeding ~ 0.5 Å required inclusion of a new Ga component shift -0.50 ± 0.03 eV, labeled 3 in Fig. 1. This new peak provides direct evidence for new Ga bonding configuration. It is not related to Ga aggregates because a shift of -0.9 eV would be expected for pure Ga. Instead it corresponds to Ga atoms mixed with Ti at the interface.[15] Component 3, present at 0.5 Å, the lowest coverage studied, increases gradually in intensity, reaches a maximum at 6 Å, and then decays very slowly. At higher coverages, it dominates the spectra but it shifts steadily to lower relative binding energy. In the low-coverage regime, component 3 is less well resolved and contains contributions from atoms bonded in many different interface chemical configurations, as evidenced by the broad peak at 2 Å. With increasing deposition, the fitting required a Doniach-Sunjic asymmetry parameter of 0.12, typical of metallic screening of core holes.[16] Component 3 for all spectra for $\Theta > 2$ Å were fitted with the DS line shape. For the highest coverage (20 Å), its resolved spin-orbit splitting indicates a well-defined Ga environment, consistent with Ga and P dilution in Ti, and it exhibits a final shift of 1.58 eV.

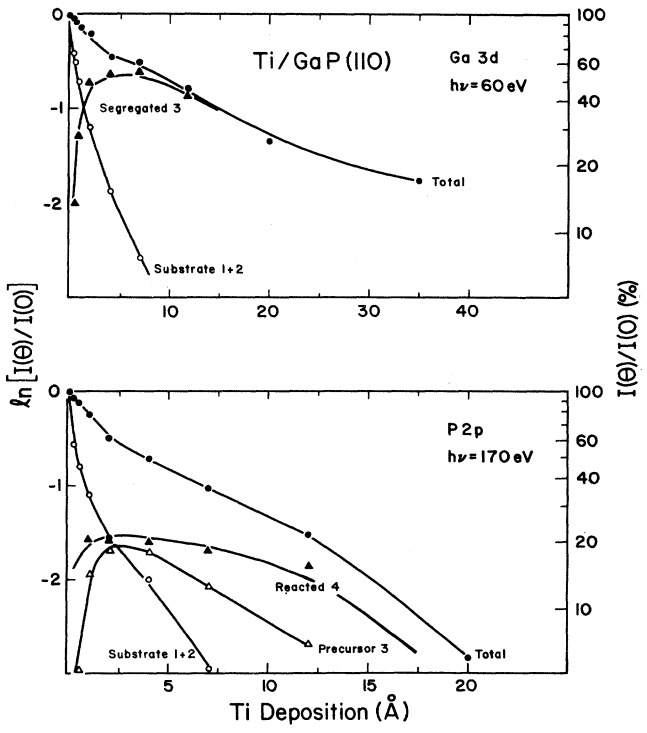

FIG. 2. Normalized core-level emission intensities (attenuation curves) showing changes in Ga $3d$ and P $2p$ content of the probed region as a function of Ti coverage. For Ga the strong reaction of Ti with the substrate is evident by the fast decay of the substrate component at low coverages. For P the total attenuation curve shows the behavior of the substrate, the transition region, and the phosphide reaction product.

These results suggest that the Ga atoms are in environments that change progressively with Ti deposition, but also that the range of Ga environments is relatively small. Analogous behavior has been observed for Ti/GaAs interfaces. It has generally been interpreted as progressive dilution of Ga in a metal-rich matrix.[15,17,18]

Inspection of the P $2p$ core-level results of Fig. 1 shows that subangstrom Ti depositions result in broadening and the loss of the surface component. This broadening was caused by the formation of two distinct reaction products. One (labeled component 3 in Fig. 1) is represented by a spin-orbit doublet shifted -0.87 ± 0.03 eV. The second component, labeled 4, appears at -0.40 ± 0.03 eV and is degenerate with the surface component at low coverages. At low coverage, component 4 can be unambiguously associated with a new feature because the surface component for Ga (and therefore P) is negligible above ~ 2 Å. Analogous results have been obtained for Ti/InP(110) where the second reacted component was degenerate with the bulk emission.[19] Component 4 dominates above ~ 4 Å. The coverage range over which component 3 appears suggests that it is due to P atoms in a transition stage from the substrate to the formation of a stable phosphide, analogous to the precursor or transition region previously observed for Ti/Si and Ti/InP.[19,20]

Figure 2 shows the total and component-specific intensities attenuation curves based on Ga $3d$ (top) and P $2p$ (bottom) emission for Ti/GaP(110). Note that the horizontal (deposition) scale for Ga is twice that for P. The P $2p$ attenuation curve shows the reduction in substrate components (components 1 and 2) with a $1/e$ length of 2.5 Å, a value much smaller than the photoelectron mean free path of 4 Å and consistent with chemical conversion of semiconductor atoms at the surface into atoms bonded differently. For P, the first reacted or precursor component, labeled 3, rises with increasing Ti deposition to a maximum at ~ 2 Å and is then attenuated with a relatively gradual $1/e$ decay length of ~ 8 Å. Component 4 reaches a maximum at ~ 4 Å and then attenuates slowly. The inflection for the substrate component reflects reduced Ti-induced disruption after an average of ~ 3 Å, consistent with kinetic constraints. From Fig. 2, it can be seen that the total P signal after 20-Å deposition is equal to $\sim 5\%$ of the clean-surface value. In contrast, a simple calculation based on the photoelectron mean free path predicts that the signal would be reduced to this value by 3λ or 12 Å. We conclude that Ti-induced disruption of the surface leads to atom rearrangement and rebonding, with most of the P atoms being retained near the buried interface.

Figure 2 also shows that the attenuation of the Ga $3d$ substrate component is approximately exponential with a $1/e$ length of ~ 2.5 Å (as for the P substrate since the two

are coupled). In contrast, the Ga 3*d* total emission persists at a much higher level than for P, with ~15% of the clean-surface value after 35-Å Ti deposition. This indicates that Ga atoms that are disrupted from the substrate segregate to the surface or near-surface region of the thickening film. Such redistribution is consistent with the observed sharpening of the Ga 3*d* emission (Fig. 1). In turn, it demonstrates an apparent reduction in the number of bonding configurations for outdiffused Ga in a Ti matrix where the line shape is best described by a Doniach-Sunjic form because of metallic screening.

These Ti/GaP results also show that there is no critical Ti coverage below which interface reaction is suppressed. The behavior at high coverage indicates approximately uniform overlayer growth, despite substrate disruption and Ga segregation. Similar conclusions can be drawn from results for Ti/GaAs and Ti/InP,[15,17–20] as explained in the Discussion section.

Pd/GaP(110)

The results for Pd/GaP(110) exhibit quite different reaction and evolution from that of Ti/GaP(110). As shown on the right of Fig. 3, the deposition of 1 Å of Pd disrupts the substrate, reduces the intensity of the surface-shifted component, and produces chemically shifted features on the high-binding-energy side of the P substrate component (labeled 3, shifted 0.36±0.03 eV with Gaussian width 710 meV at 1-Å Pd deposition). The relative binding position energy of component 3 varies with deposition but stabilizes at 0.46±0.03 eV after 4 Å Pd (width ~630 meV). Such behavior generally indicates that distinct bonding configurations form but that they start off in a mixed state involving atoms released from the disrupted substrate. The deposition of ~4 Å of Pd gives rise to a second P 2*p* component, labeled 4, shifted 0.98±0.03 eV relative to the substrate. These two P 2*p* interface components dominate at higher coverage, and the contribution from the substrate is small by ~10 Å (photoelectron mean free path 4 Å).

The bottom portion of Fig. 4 shows the attenuation of the total and specific P 2*p* features. The total P emission first decreases rapidly, exhibits a plateau region, and decreases rather slowly (1/*e* length 45 Å). The component-specific attenuation curves show the increase in intensity of the two Pd-induced components and their very slow, but approximately parallel, reduction after ~10 Å.

The results of Figs. 3 and 4 make it possible to describe the progressive redistribution of P atoms across the interfacial region. Pd deposition initially induces disruption, and the appearance and persistence of components 3 and 4 demonstrate that the atoms responsible for 3 and 4 outdiffuse to the surface and near-surface region. At high coverages, component 3 would be associated with surface segregated P atoms while component 4 corresponds to P atoms intermixed with Pd near the surface. The parallel attenuation of the two chemically shifted components suggests that the region probed by photoemission remains almost unchanged after ~20 Å of Pd have been deposited, with changes that reflect the progressive retention (dissolving) of P in the thickening Pd layer. There is certainly no evidence for the strong chemical trapping of P that was apparent for Ti/GaP or Ti/InP.[19]

Figure 3 also shows representative Ga 3*d* core-level EDC's taken with high-surface sensitivity at $h\nu=60$ eV ($\lambda\sim4$ Å). Component 3 appears at -0.56 ± 0.03 eV during the early stages of interface development and gradually sharpens with increased Pd deposition (Gaussian width 467 meV at 1 Å versus 341 meV at 40 Å). At high coverage, there is only a single distinct configuration as Ga is dissolved in the Pd layer and, as for Ti, it was best fit with a Doniach-Sunjic line shape with $\alpha\sim0.10$ because of metallic screening of the core hole.

The results of Figs. 3 and 4 indicate that component 2, which is initially due to surface-shifted atoms, can be observed for Pd depositions as high as ~8 Å. Since there is no evidence for the exposure of large amounts of surface region, we conclude that a new bonding configuration develops with a binding energy that cannot be resolved

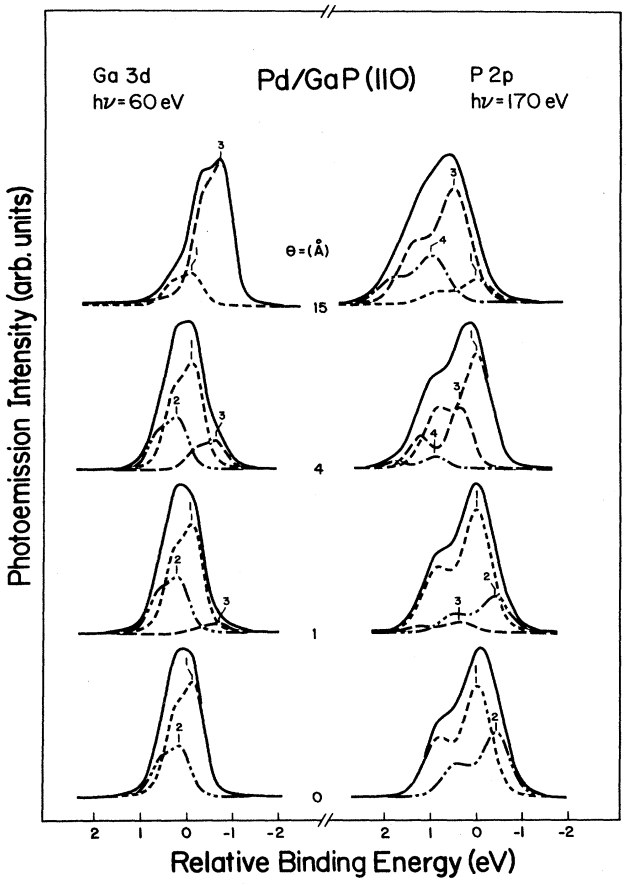

FIG. 3. Representative Ga 3*d* and P 2*p* EDC's analogous to those of Fig. 1. For Ga, component 1 corresponds to bulk atoms, component 2 to surface atoms, and component 3 to Ga atoms dissolved into the Pd overlayer. For P, components 3 and 4 reflect P atoms released into the Pd overlayer. The dominance of component 3 at high coverages indicates that component 3 represents surface-segregated atoms and component 4 atoms dissolved in the overlayer.

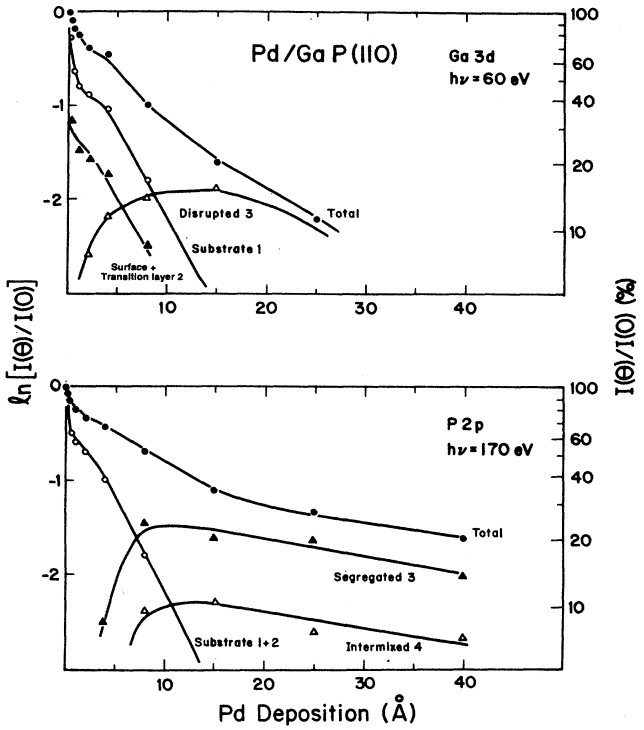

FIG. 4. Total and component-specific attenuation curves for Pd/GaP(110). The substrate attenuation can be followed from the Ga 3*d* signal along with the contribution from the transition layer (component 2) presented in Fig. 3. The attenuation signal of Ga is faster than that of P, showing that P outdiffuses into the overlayer much more readily than Ga atoms.

from the surface-shifted component. Analogous results have been found for the cations for Pd overlayer formation on GaAs, InP, and InSb.[21] The intensity of this component can be estimated by considering the rate at which the surface component for P is lost during Pd deposition, with the results shown in Fig. 4. As shown, this component attenuates with a rate that is equal to the substrate. We associate it with a transition layer or interface layer between the adatoms and the undisrupted substrate. Increased deposition leads to the burial of this layer by a region of intermixed Pd, P, and Ga atoms.

Comparison of the Ga and P results of Fig. 4 suggests that the distribution of Ga atoms is simpler than that for P because P atoms segregate and float during Pd overlayer formation. These results are different from those for Ti/GaP(110) because a stable Ti—P bonding configuration forms and its growth leads to the ejection of the Ga cations. The Ga and P results for Pd/GaP are similar to those found for Pd/GaAs and Pd/InP.[18,21,22]

Ag/GaP(110) and Au/GaP(110)

The results for Au/GaP(110) indicate substantial Au-induced substrate disruption, as seen by representative Ga 3*d* and P 2*p* core-level EDC's of Fig. 5. For Ga 3*d*, the substrate features are attenuated and a chemically shifted component due to intermixed Ga in the Au overlayer dominates by ~10 Å (shifted −0.36±0.03 eV). For coverages between 40 and 80 Å of Au, the Ga feature sharpens due to the convergence of the Ga local chemical environment to a single configuration and the line shape exhibits an asymmetry characteristic of metallic screening (asymmetry factor $\alpha=0.10$).

Au-induced changes in the P 2*p* line shape are not as easily distinguished, but consistent line-shape analysis makes it possible to resolve two components, as shown at the right of Fig. 5. Component 3 appears at ~0.5 Å at 0.38±0.03 eV and component 4 appears at ~4 Å at 0.55±0.03 eV higher binding energy than component 3. They dominate after ~10-Å deposition, and their persistence at high coverage indicates P atom segregation to the surface and near-surface regions. We associate component 3 with segregated P on the surface and component 4 with atoms within the Au overlayer (intermixed). Their different Au coordination then makes

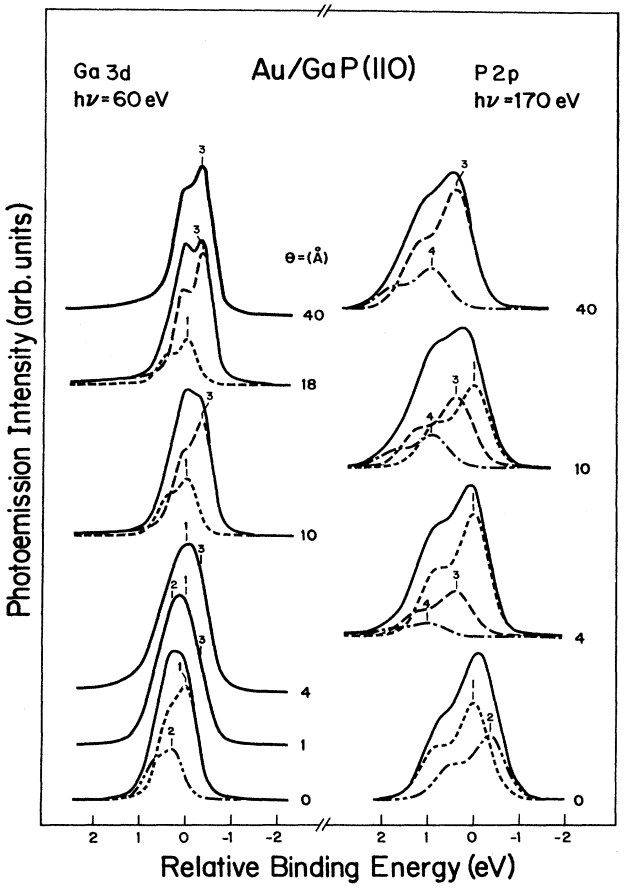

FIG. 5. Core-emission spectra of Ga 3*d* and P 2*p* for the Au/GaP(110) interface, similar to those of Figs. 1 and 3. For Ga, component 3 corresponds to Ga atoms dissolved in the overlayer. For P, components 3 and 4 correspond to P atoms segregated to the surface and dissolved in the overlayer, respectively.

them distinguishable, as was the case for P in Pd/GaP or Pd overlayer growth on InP(110), GaAs(110), and InSb(110).[21] The expulsion of P to the Au surface is consistent with the small heats of formation calculated for Au—P bonds.[23]

Inspection of the valence-band spectra for Au/GaP(110) reveals that the characteristic splitting of the Au 5*d* band gradually increases from a value typical for dispersed atoms but does not reach the bulk value by 40-Å deposition. This, together with the Ga 3*d* and P 2*p* core-level line shapes, indicates that Au adatoms do not aggregate to form large three-dimensional clusters at low coverage. The high coverage Au valence-band features suggest the presence of Ga and P atoms in the probed surface and near-surface region. This is confirmed from the total attenuation curves for Ga and P, as summarized in Fig. 6. Hence, the effect of Au condensation is the disruption of Ga and P atoms from the substrate such that these atoms partly dissolve in the Au matrix and partly segregate to the Au surface. As the overlayer thickens, the segregated atoms continue to float on the surface, and their presence is readily detected in the core-level and valence-band photoemission spectra. These results are very similar to those obtained for Au deposition onto GaAs(110) and InP(110) (Refs. 24–30), as well as for Si(111) (Refs. 31–34), and Ge(111) (Ref. 35).

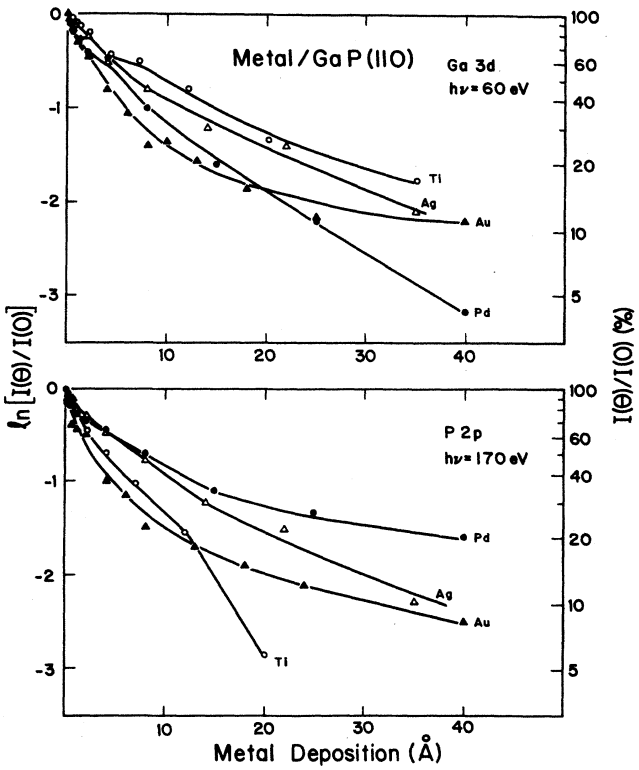

FIG. 6. Summary of attenuation curves for the total surface-sensitive Ga 3*d* and P 2*p* emission showing that Ga is dissolved the greatest in Pd and the least for Ti. For P, the trend is reversed with the greatest expulsion being observed for Pd overlayers and the least for Ti because of reaction with Ti to form a stable phosphide.

Silver vapor deposition onto GaP(110) at 300 K gives rise to only slight line-shape changes in the Ga 3*d* and P 2*p* core-level EDC's (depositions to 80 Å, not shown). Intensity analysis shows that the ratio I_{surf}/I_{bulk} decreased very slowly with Ag deposition for both Ga 3*d* and P 2*p*, with almost no change at low coverage. Valence-band spectra show the distinctive Ag Fermi-level step, and the 5*d* band resembles that of bulk Ag after the deposition of ~2 Å. As shown in Fig. 6, the total Ga and P attenuation is very slow. We conclude that Ag grows in a three-dimensional cluster mode on GaP(110) and that no detectable substrate disruption occurs. The inert behavior of Ag toward reaction with covalent semiconductor surfaces and its tendency to spontaneously cluster at 300 K have been reported for almost all interfaces studied.[22,36–41]

DISCUSSION

The total attenuation curves for Ti, Pd, Ag, and Au deposition onto GaP(110) are summarized in Fig. 6 based on surface-sensitive spectra. For Ti, there is evidence for phosphide formation and the expulsion of the cation Ga. For Pd and Au, there is no evidence for the formation of stable *M* phosphides and, as a result, P is expelled to the surface. These trends agree well with the heats of formation of P with Ti, Pd, and Au.[23] The heat of formation is largest for Ti, suggesting the formation of a stable phosphide. The Ga 3*d* emission for Pd indicates that Ga is intermixed in the metallic overlayer, as evidenced by the much faster attenuation for Pd overlayers than for Ti or Au. For Au, substrate disruption results in the intermixing of both Ga and P as well as partial segregation, without the formation of Au-Ga or Au-P phases. For Ag, the results are typical of clustering, and there is no evidence for reaction. This is also consistent with the calculated heats of formation and solution for Ag since there are no favorable Ag-P or Ag-Ga compounds.[23,42]

These results can best be viewed in the context of equivalent experiments with the more extensively studied *M*/GaAs(110) and *M*/InP(110) interfaces where *M* denotes Ti, Pd, Ag, and Au and where other adatoms have been examined as well. If we compare the behavior of the anion and cation, we find the following important trends.

Ti adatom deposition onto cleaved surfaces of each of these semiconductors leads to Ti-anion bond formation, and the same is true for other highly reactive adatoms. The result of this process is the nucleation of reacted clusters and expulsion of the cation as the reacted clusters grow, a process which appears even for clusters of very small dimension. For Ti/InP, reaction is particularly strong, and In atoms are expelled and segregate to the surface because of its very low solubility in either TiP or Ti. (The low-coverage onset of the expulsion process was recently reported for Co/InP interfaces.[43]) For Ti/GaAs and Ti/GaP, Ga atoms released from the substrate are also expelled from the Ti-anion cluster, as reflected by detailed temperature-dependent and sputter-profiling experiments for metal overlayers on GaAs, but Ga is also ob-

served to intermix in the growing metal overlayer.[44] This intermixing reflects the greater Ga solubility or tendency to form bonds compared to In.

Comparison of the atomic distributions for (Pd,Au)–III-V compound semiconductor interfaces with those for more reactive metals (e.g., Ti, Cr, Co, and Fe) shows the common behavior of adatom-induced substrate disruption and the release of substrate atoms. The reactive metals form stable compounds with the anions, expelling the cation. For Pd and Au, the adatoms do not form strong bonding configurations and the released semiconductor atoms are distributed through surface and near-surface segregation. This cation segregation is regulated by kinetics and the nonequilibrium trapping of Ga, In, and P atoms in the Pd or Au film.

In a recent study of the Au/InP interface, Waddill *et al.*, were able to study the kinetics of interface formation by comparing Au adatom deposition of 300 and 60 K.[30] Significant differences in interface morphology were found for Au deposition at 300 K and resulted in a thick Au overlayer containing intermixed In and P, analogous to that discussed here for Au/GaP. The same amount of substrate disruption was observed at 60 K, but surface segregation was almost completely inhibited. This further demonstrates that the kinetics controlling diffusion of the cation and anion in the growing metal overlayer control atom distribution in the thickening overlayer.

Ag adatom deposition onto cleaved surfaces of GaP leads to no apparent disruption and the formation of clusters. Similar results have been obtained for room-temperature deposition of Ag/GaAs interfaces, where only a weak interaction with substrate was noted.[37–39] For Ag/InP, Ag interacts slightly with the substrate and the results show some In intermixed at intermediate coverages.[36] In all cases, these clusters quickly assume metallic character, but cover the surface rather ineffectively with long $1/e$ decay lengths. However, recent low-temperature studies of Ag/GaAs demonstrated a more nearly layer-by-layer growth consistent with reduced Ag adatom surface mobility and the inhibition of Ag cluster formation.[39–41] These results showed evidence of an interface component that was assigned to a distinct interface state. The results at 300 K could also contain such features, although none were apparently observed. Such low-temperature results indicate the possibility of altering the interface morphology by limiting the kinetics at the interface.

Finally, these results indicate that, once disruption occurs, the behavior of Ga and P atoms released from the semiconductor are the same, regardless of whether the semiconductor is GaP, InP, or GaAs. It should then be clear that the deposition process itself leads to limited reaction or disruption, but that the solubility or reactivity of the released atoms in the overlayer then controls their redistribution. Likewise, the effects that would be observed at higher or lower temperature would also be analogous, with annealing providing the energy needed for mass transport and continued reaction and cooling providing a kinetic barrier against either reaction or segregation.

ACKNOWLEDGMENTS

This work was supported by the Army Research Office under Contract No. ARO DAAL03-88-K-0093. We are grateful to the Optoelectronics Division of Hewlett Packard and, in particular, to Dr. D. Vanderwater for generously providing the GaP crystals. The photoemission experiments were conducted at the Wisconsin Synchrotron Radiation Center, which is supported by the National Science Foundation, and the support of the personnel of that facility is gratefully acknowledged. Data analysis was greatly facilitated by access to IBM PC-RT's provided through an IBM Materials Science and Processing Grant. The authors thank R. L. Siefert for helping in the core-level analysis.

---

*Present address: Department of Physics, University of Calabria, 87030 Roges di Rende (CS), Italy.

[1]See the following for reviews of photoemission results for a variety of metal-semiconductor interfaces: D. M. Hill, F. Xu, Z. Lin, and J. H. Weaver, Phys. Rev. B **38**, 1893 (1988); L. J. Brillson, Surf. Sci. Rep. **2**, 123 (1982); W. E. Spicer, T. Kendelewicz, N. Newman, K. K. Chin, and I. Lindau, Surf. Sci. **168**, 240 (1986). R. H. Williams, in *Physics and Chemistry of III-V Compound Semiconductor Interfaces,* edited by C. W. Wilmsen (Plenum, New York, 1985); R. Ludeke, Surf. Sci. **168**, 291 (1986).

[2]For a good review of the information gained by other techniques, see L. C. Feldman and J. W. Mayer, *Fundamentals of Surface and Thin Film Analysis* (North-Holland, New York, 1986).

[3]D. E. Aspnes, C. G. Olson, and D. W. Lynch, Phys. Rev. B **14**, 2534 (1976).

[4]F. Sette, P. Perfetti, F. Patella, C. Quaresima, C. Capasso, M. Capozi, and A. Savoia, Phys. Rev. B **28**, 4882 (1983).

[5]P. Chiaradia, L. J. Brillson, M. Slade, R. E. Viturro, D. Kilday, N. Tache, M. Kelly, and G. Margaritondo, J. Vac. Sci. Technol. B **5**, 1075 (1987).

[6]I. M. Vitomirov, C. M. Aldao, M. Schabel, G. D. Waddill, S. G. Anderson, and J. H. Weaver, J. Vac. Sci. Technol. A **7**, 758 (1989).

[7]A. B. McLean and R. Ludeke, Phys. Rev. B **39**, 6223 (1989).

[8]P. Chiaradia, M. Fanfoni, P. Nataletti, P. De Padova, L. J. Brillson, M. L. Slade, R. E. Vitturo, D. Kilday, and G. Margaritondo, Phys. Rev. B **39**, 5128 (1989).

[9]F. Xu, C. M. Aldao, I. M. Vitomirov, Z. Lin, and J. H. Weaver, Phys. Rev. B **36**, 3495 (1987).

[10]G. K. Wertheim and S. B. Dicenzo, J. Electron. Spectrosc. Relat. Phenom. **37**, 57 (1985).

[11]J. J. Joyce, M. del Giudice, and J. H. Weaver, J. Electron Spectrosc. Relat. Phenom. **49**, 31 (1989) discusses the lineshape analysis procedures.

[12]D. E. Eastman, T.-C. Chiang, P. Heimann, and F. J. Himpsel, Phys. Rev. Lett. **45**, 656 (1980).

[13]W. Mönch, Solid State Commun. **58**, 215 (1986).
[14]C. Priester, G. Allan, and M. Lannoo, Phys. Rev. Lett. **58**, 1989 (1987).
[15]R. Ludeke, D. Straub, F. J. Himpsel, and G. Landgren, J. Vac. Sci. Technol. A **4**, 874 (1986).
[16]S. Doniach and M. Sunjic, J. Phys. C **3**, 285 (1970).
[17]M. W. Ruckman, M. del Giudice, J. J. Joyce, and J. H. Weaver, Phys. Rev. B **33**, 2191 (1986).
[18]R. Ludeke and G. Landgren, Phys. Rev. B **33**, 5526 (1986).
[19]C. M. Aldao, I. M. Vitomirov, F. Xu, and J. H. Weaver, Phys. Rev. B **37**, 6019 (1988).
[20]M. del Giudice, J. J. Joyce, M. W. Ruckman, and J. H. Weaver, Phys. Rev. B **35**, 6213 (1987).
[21]I. M. Vitomirov, C. M. Aldao, Z. Lin, Y. Gao, B. M. Trafas, and J. H. Weaver, Phys. Rev. B **38**, 10 776 (1988).
[22]T. Kendelewicz, W. G. Petro, I. Lindau, and W. E. Spicer, J. Vac. Sci. Technol. B **2**, 453 (1984).
[23]The experimentally obtained heat of formation for Au_2P_3 is -99.6 kJ/mol, much smaller than the value for TiP, -282.8 kJ/mol [see NBS Tables of Chemical Thermodynamical Properties, J. Phys. Chem. Ref. Data **11**, Suppl. 2 (1982)]; O. Kubachewski and C. B. Alcook, *Metallurgical Thermochemistry* (Pergamon, Oxford, 1979).
[24]F. Xu, Y. Shapira, D. M. Hill, and J. H. Weaver, Phys. Rev. B **35**, 7417 (1987).
[25]M. Grioni, J. J. Joyce, and J. H. Weaver, J. Vac. Sci. Technol. A **4**, 964 (1986).
[26]P. W. Chye, I. Lindau, P. Pianetta, C. M. Garner, C. Y. Su, and W. E. Spicer, Phys. Rev. B **18**, 5545 (1978); W. G. Petro, I. A. Babalola, T. Kendelewicz, I. Lindau, and W. E. Spicer, J. Vac. Sci. Technol. A **1**, 1181 (1983); W. G. Petro, T. Kendelewicz, I. Lindau, and W. E. Spicer, Phys. Rev. B **34**, 7089 (1986).
[27]Y. Shapiro, L. J. Brillson, A. D. Katnani, and G. Margaritondo, Phys. Rev. B **30**, 4856 (1984).
[28]I. A. Babalola, W. G. Petro, T. Kendelewicz, I. Lindau, and W. E. Spicer, J. Vac. Sci. Technol. B **2**, 453 (1984).
[29]L. J. Brillson, C. F. Brucker, A. D. Katnani, N. G. Stoffel, and G. Margaritondo, J. Vac. Sci. Technol. **19**, 661 (1981).
[30]G. D. Waddill, C. M. Aldao, I. M. Vitomirov, Y. Gao, and J. H. Weaver, J. Vac. Sci. Technol. A **1**, 865 (1989).
[31]F. Xu, C. M. Aldao, I. M. Vitomirov, and J. H. Weaver, Appl. Phys. Lett. **51**, 1946 (1987).
[32]L. Braicovich, C. M. Garner, P. R. Skeath, C. Y. Su, P. Y. Chye, I. Lindau, and W. E. Spicer, Phys. Rev. B **20**, 5131 (1979).
[33]A. Franciosi, D. G. O'Neill, and J. H. Weaver, J. Vac. Sci. Technol. B **1**, 524 (1984).
[34]L. J. Brillson, A. D. Katnani, M. Kelly, and G. Margaritondo, J. Vac. Sci. Technol. A **2**, 551 (1984).
[35]M. W. Ruckman, J. J. Joyce, F. Boscherini, and J. H. Weaver, Phys. Rev. B **34**, 5118 (1986).
[36]W. G. Petro, T. Kendelewicz, I. A. Babalola, and W. E. Spicer, Mat. Res. Soc. Symp. Proc. **25**, 329 (1984); I. A. Babalola, W. G. Petro, T. Kendelewicz, I. Lindau, and W. E. Spicer, Phys. Rev. B **29**, 6614 (1984).
[37]R. Ludeke, T.-C. Chiang, and T. Miller, J. Vac. Sci. Technol. B **1**, 581 (1983).
[38]K. K. Chin, S. H. Pan, D. Mo, P. Mahowald, N. Newman, I. Lindau, and W. E. Spicer, Phys. Rev. B **32**, 918 (1985).
[39]G. D. Waddill, C. M. Aldao, I. M. Vitomirov, S. G. Anderson, C. Capasso, and J. H. Weaver, J. Vac. Sci. Technol. (to be published) and citations therein.
[40]K. Stiles, A. Kahn, D. G. Kilday, and G. Margaritondo, J. Vac. Sci. Technol. A **5**, 987 (1987); K. Stiles and A. Kahn, Phys. Rev. Lett. **60**, 440 (1988).
[41]K. K. Chin, T. Kendelewicz, C. McCants, R. Cao, K. Miyano, I. Lindau, and W. E. Spicer, J. Vac. Sci. Technol. A **4**, 969 (1986); R. Cao, K. Miyano, T. Kendelewicz, K. K. Chin, I. Lindau, and W. E. Spicer, *ibid.* **5**, 998 (1987); W. E. Spicer, R. Cao, K. Miyano, C. McCants, T. T. Chiang, C. J. Spindt, N. Newman, T. Kendelewicz, I. Lindau, E. Weber, and Z. Liliental-Weber, in *Proceedings of the NATO Advanced Research Workshop on Metallization and Metal-Semiconductor Interfaces, Garching bei München, Germany, 1988* (Plenum, New York, 1988).
[42]A. K. Neisen, F. R. De Boer, R. Boon, P. F. de Châtel, W. C. M. Mattens, and A. R. Miedema, CALPHAD **7**, 51 (1983).
[43]F. Xu, C. M. Aldao, I. M. Vitomirov, Z. Lin, and J. H. Weaver, Phys. Rev. B **36**, 3485 (1981).
[44]F. Xu, Z. Lin, D. M. Hill, and J. H. Weaver, Phys. Rev. B **36**, 6624 (1987).